

Photoluminescence and excitation-photoluminescence study of spontaneous ordering in GaInP₂

G. S. Horner, A. Mascarenhas, R. G. Alonso, S. Froyen, K. A. Bertness, and J. M. Olson

National Renewable Energy Laboratory, Golden, Colorado 80401-3393

(Received 11 June 1993; revised manuscript received 23 September 1993)

Low-temperature polarized photoluminescence and polarized photoluminescence-excitation spectroscopies are used to probe the electronic structure of GaInP₂ epilayers grown by organometallic vapor-phase epitaxy. The epilayers were grown at various sample temperatures and exhibit different degrees of ordering. A systematic study of the absorption edge and luminescence line shapes provides evidence for a distribution of order parameters, η , within the more ordered samples of this study.

I. INTRODUCTION

The phenomenon of spontaneous ordering in ternary alloys, such as GaInP₂, has attracted considerable attention.¹⁻⁵ Of interest is the bandgap lowering that it causes, and the importance of this material for making solar cells, light emitting diodes, and semiconductor injection lasers.^{6,7} In addition, for a given value of the composition x in Ga _{x} In _{$1-x$} P, ordering allows for growth condition-dependent control of the band gap.⁸⁻¹⁰

The sample growth temperature dependence of the band gap E_g has been investigated in ordered alloys by electroreflectance,^{4,11,12} photoluminescence (PL),^{4,5,9,10,13} and excitation photoluminescence (PLE).^{13,14} Recently, a systematic piezomodulated reflectivity study of the band gap E_g , the crystal-field splitting Δ_c , and the spin-orbit splitting Δ_{SO} as a function of ordering has been carried out.¹⁵ In this paper, we present a detailed PL and PLE study on the phenomenon of spontaneous ordering in GaInP₂ epilayers grown by organometallic vapor-phase epitaxy (OMVPE). The results of this study support the preliminary findings and model of a recent paper,¹³ and we confirm that the ordered GaInP₂ epilayers in this sample set (for which growth and substrate tilt conditions are given below) do not consist of domains with a unique ordering parameter η , but that they are comprised of a statistical distribution of domains having different order parameters (Fig. 1).

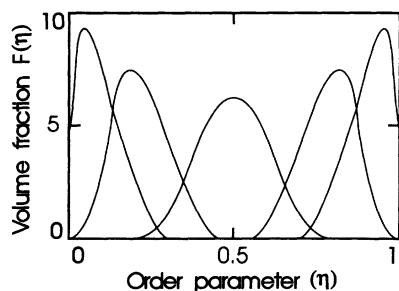


FIG. 1. Possible distributions of ordering $F(\eta)$ in GaInP₂ for various degrees of average ordering. Note that a perfectly disordered sample must be represented by a δ function at $\eta=0$, whereas partially ordered samples may be described mathematically with $F(\eta)$'s of finite width.

II. SAMPLE GROWTH AND EXPERIMENTAL SETUP

A series of GaInP₂ epilayers were grown using atmospheric pressure OMVPE in a vertical disklike reaction vessel with tangential injection lines. The substrates consist of (001) GaAs, misoriented 2° towards [011]. The various epilayers were grown lattice matched at different substrate growth temperatures T_g , ranging from 600°C to 750°C. For all samples, the growth rate was held constant at 4.4 $\mu\text{m}/\text{h}$ with a V:III inlet ratio of 50:1, corresponding to a phosphine partial pressure of 233 Pa. The resulting composition was nominally Ga_{0.505}In_{0.495}P, with a maximum deviation of $\Delta x = 0.005$.

The measured band gap is determined mainly by the degree of ordering. However, it is necessary to correct for band-gap changes due to the small composition deviations from the nominal value. The composition can be determined from the residual tetragonal deformations induced by film-substrate strain. Double-crystal x-ray diffraction was performed on the (004) reflection of all samples, giving directly the tetragonality $c/a - 1$ of the film.¹⁶ To account for composition-induced changes in E_g , we used the measured E_g for a set of samples of vary-

TABLE I. Parameters of the OMVPE grown Ga_{0.5}In_{0.5}P/GaAs epilayers which were investigated. T_g is the growth temperature and E_g is the band gap measured by photoluminescence at 15 K (the peak luminescence energy shows no polarization dependence at low temperatures). The transition energies were corrected for composition as described in the text.

Sample	T_g (°C)	E_g (eV)
K-121	750	1.982
K-078	750	1.982
K-063	730	1.945
K-174	730	1.951
K-128	715	1.930
K-148	700	1.914
K-075	670	1.892
K-044	630	1.912
K-134	630	1.907
K-175	600	1.969

ing compositions versus $c/a - 1$. We then corrected E_g by the appropriate energy shift required to produce $c/a = 1$ at growth temperature. All corrections are less than 5 meV.

The PL emission spectra were analyzed with a linear polarizer, \mathbf{P} , oriented either parallel or perpendicular to the $[1\bar{1}0]$ direction, where $[1\bar{1}0]$ is the projection of the CuPt B -variant ($[1\bar{1}1]$ or $[\bar{1}11]$) ordering axis on the (001) sample surface. The PLE spectra were collected without an emission polarizer, but the polarization of the incident laser was selected to be either along the $[110]$ or the $[1\bar{1}0]$ direction. In the PLE experiments, the spectrometer was set at the low-energy tail of the PL peak, and the incident wavelength of a dye laser was scanned. The samples studied and their growth temperatures are indicated in Table I. All epilayers are 0.3 mm thick, and they are not intentionally doped.

III. EXPERIMENTAL RESULTS AND DISCUSSION

In Fig. 2 we show characteristic PL and PLE spectra for a sample that exhibits a high degree of ordering (K -134, $T_g = 630^\circ\text{C}$) and one that exhibits a low degree of ordering (K -121, $T_g = 750^\circ\text{C}$). The spectra were obtained at 15 K. The PL and PLE polarizations are indicated in the figure. A number of trends, which we outline below, can be extracted from these spectra.

We first focus on Fig. 2(a), which shows the PL and PLE spectra for the ordered sample. The energy

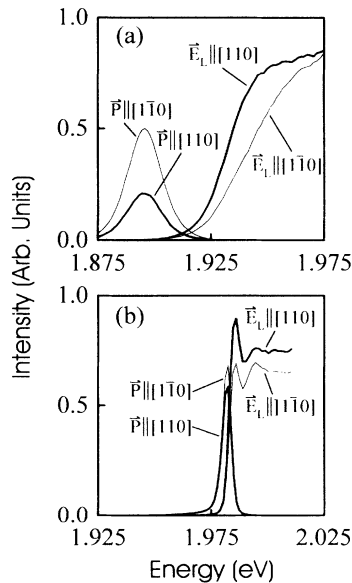


FIG. 2. PL and PLE spectra measured at 15 K for (a) an ordered sample (K -134, $T_g = 630^\circ\text{C}$) and (b) a disordered sample (K -121, $T_g = 750^\circ\text{C}$). The PL emission spectra (labeled \mathbf{P}) were collected with a linear polarizer oriented along the indicated crystallographic direction. No emission polarizer was used for the PLE measurements, but the incident laser polarization was varied between the $[110]$ and $[1\bar{1}0]$ directions (as indicated by the \mathbf{E}_L label).

difference of the position of the PLE edge for both polarizations is attributed to the crystal-field splitting Δ_c in the ordered sample.¹⁷ An energy splitting of the absorption edge in polarized PLE measurements is to be expected based on the band-structure and polarization selection rules, as discussed previously.¹³ From the spectra we deduce a half maximum splitting of $\Delta_c = 9$ meV, which is consistent with previous polarized piezomodulated reflectivity results on the same sample.¹⁵ The PL at 15 K shows no polarization energy shift. This is because PL involves the product of a density of states term with a Boltzmann factor term and the latter at low temperatures tends to favor recombination from the lowest energy transition. At room temperature, however, the effect of the Boltzmann factor is not so prominent and so an energy splitting between the polarizations is apparent in the PL spectrum (the temperature dependence of the energy of the PL peaks is given below in Fig. 3). PLE, being related to absorption (i.e., to the upward transition), exhibits the crystal-field splitting at all temperatures.

In Fig. 2(a) we also note a large redshift of the PL peak with respect to the PLE rising edge. Within the framework of our model,¹³ which considers a statistical distribution of domains $F(\eta)$, the redshift arises from the fundamental difference between an absorption process (PLE) and an emission process (PL) at low temperature. In the absorption process, the dominant contribution occurs from regions near the peak of the $F(\eta)$ distribution. In the emission process, however, electrons tend to drift to domains with lower band gaps (larger order parameter, η), and then recombine, and hence the dominant contribution occurs from regions characterized by the low- E_g side of the $F(\eta)$ distribution. At room temperature, this effect of the Boltzmann factor is diminished, thus reducing the redshift (this is observed in Fig. 3).

Figure 2(b) shows the PL and PLE spectra for the disordered sample. As expected, a disordered sample exhibits a zinc-blende type of symmetry and the PLE spectra yields a very small crystal-field splitting $\Delta_c < 1$ meV. This value is also consistent with previous piezomodulated reflectivity results.¹⁵ In addition, the PL peak has the same energy as the PLE edge: that is, it has a negligible redshift. Following our interpretation based on the distribution of ordered domains (Fig. 1), this indicates that in disordered samples the distribution function $F(\eta)$ approaches a δ function centered at $\eta_p = 0$. This is also confirmed by the fact that the width of the PL peaks are narrower in the disordered sample, as compared to the ordered one (this is discussed in more detail later in relation to Fig. 8). The same effect has also been seen in other samples.⁵ Furthermore, the rising edge of the PLE is sharper in the disordered sample as compared to the more ordered sample, consistent with the statistical distribution of band gaps within the laser sampling volume [see Figs. 2(a) and 2(b)].¹³

Figure 3 shows the temperature dependence of polarized PL in samples with various degrees of ordering. As explained above, the polarization splitting increases with increasing temperature, the splitting being larger for the most ordered sample in Fig. 3(c), and negligible for the least ordered sample in Fig. 3(a).⁴ Consistent with the

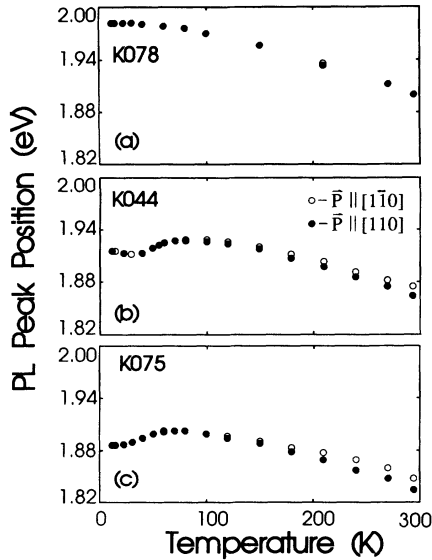


FIG. 3. Temperature dependence of polarized PL in samples with various degrees of ordering. Plots (a), (b), and (c) correspond to very low, medium, and significant degrees of ordering, respectively. Although only high-power data are shown for comparison's sake, (c) shows a strong dependence of low-temperature behavior on incident laser power density. This is consistent with a low density of states associated with the low-energy tail of the $F(\eta)$ distribution.

argument based on the effect of the Boltzmann factor, the splitting slowly increases in the range 0–293 K, or 26 meV of thermal energy, which corresponds approximately to the value of Δ_c . Below 60 K we observe a sudden redshift in the energy of the PL peak in the ordered samples, which is due to the drift of electrons into the more ordered domains of $F(\eta)$. It is assumed that the electron-hole pair has a sufficient lifetime at low temperature to drift to neighboring regions which have a lower band gap. Figure 3 indicates that the redshift of PL with respect to PLE occurs predominantly below 60 K, and that it is larger for more ordered samples.

In the partially ordered samples of this study, the magnitude of the low-temperature PL redshift is dependent upon the incident laser power. If we photoexcite a large population of electron-hole pairs with a high incident power density (not shown), then the anomalous low-temperature behavior of Figs. 3(b) and 3(c) is mitigated, and these samples more closely exhibit the temperature behavior of the disordered alloy [Fig. 3(a)]. This is consistent with our $F(\eta)$ distribution function: the low band-gap (high η) tail of the $F(\eta)$ distribution represents a smaller density of states. As we increase the laser power density, the lowest energy recombination paths become saturated, and the luminescence occurs predominantly from higher energy states which exhibit an order parameter closer to $\eta = \eta_p$.

We now focus on the trends of our experimental data as a function of the degree of ordering. The PL band gap at 60 K, $E_g(60\text{ K})$, is used as an indication of the degree of ordering; the lower the band gap, the higher the order

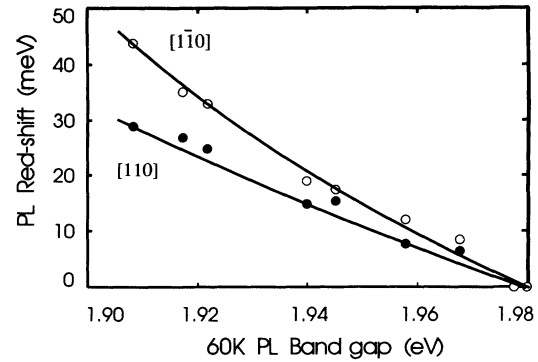


FIG. 4. Redshift of the PL peak with respect to the PLE edge vs $E_g(60\text{ K})$ as measured by PL. The curves for the different polarization are labeled [110] and $[1\bar{1}0]$. The more ordered samples exhibit a significantly larger low-temperature redshift.

parameter η_p . Although η_p has not been measured directly, theoretical relations between E_g and η_p have been developed.¹ Figure 4 shows the redshift of the PL with respect to the PLE edge at 15 K vs $E_g(60\text{ K})$. The redshift of the PL relative to the PLE increases with ordering, consistent with an increasing width of $F(\eta)$ with increasing η_p . We note again that the redshift is explained on the basis of a distribution of ordering parameters: the PLE signatures probe the peak of the distribution while PL probes the more ordered regions which comprise the right-hand side tail of the distribution (Fig. 1). The energy separation between the curves for [110] and $[1\bar{1}0]$ polarization indicates how the crystal-field splitting increases with increasing ordering. At 15 K, PL does not show significant polarization dependence, whereas the PLE does show clear polarization dependence.

Figure 5 shows the PLE polarization splitting at 15 K as a function of $E_g(60\text{ K})$. The PLE splitting is attributed to the crystal-field splitting caused by ordering. The results compare favorably with crystal-field splitting

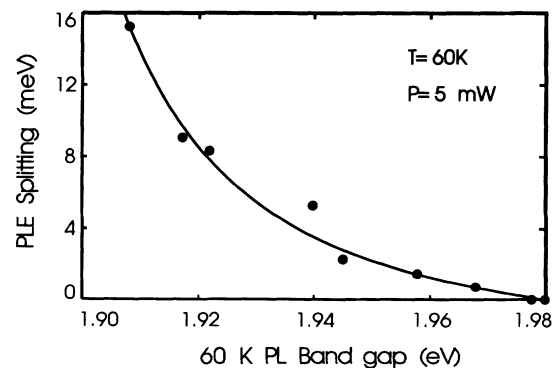


FIG. 5. PLE polarization splitting as a function of a 60-K photoluminescence band gap. The PLE splitting is defined as the energy difference between the two polarizations of the absorption edge half maximum.

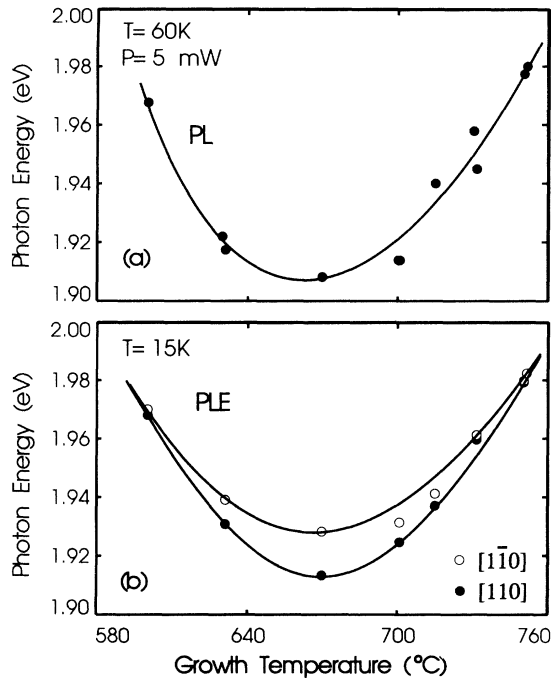


FIG. 6. (a) Energy of the PL peak at 60 K as a function of sample growth temperature T_g . (b) Energy of the PLE edge (half maximum) at 15 K as a function of sample growth temperature T_g , for both incident polarizations. Both measurements exhibit the characteristic U shape, but the polarized PLE measurements directly show the presence of the crystal-field valence-band splitting in the more ordered samples.

versus E_g measurements done by piezomodulated reflectivity¹⁵ at the same temperature.

Next, we focus on trends as a function of sample growth temperature T_g . Figure 6(a) shows the energy of the PL peak at 60 K as a function of sample growth temperature. A characteristic U -shaped curve is observed,

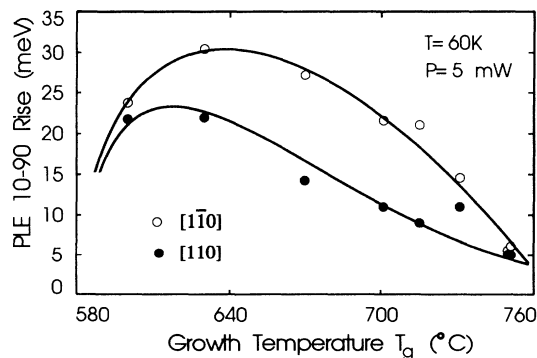


FIG. 7. Slope of the PLE as a function of growth temperature T_g , the slope being measured as the energy width of the 10–90% intensity rise. The labels [110] and $[1\bar{1}0]$ indicate the polarization of the incident light. The PLE slope is controlled by the distribution of order parameters within the volume being probed, as well as the presence of the crystal-field splitting in the more ordered samples.

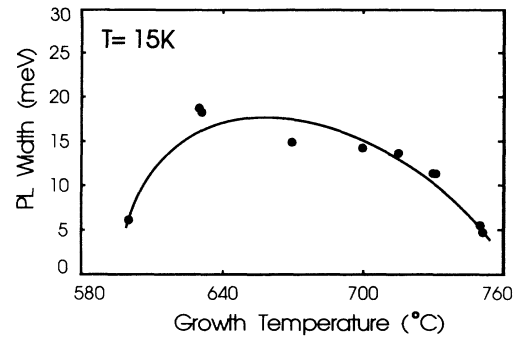


FIG. 8. Plot of the width of the PL peak as a function of growth temperature T_g . The PL width is expected to give an indication of the width of the distribution $F(\eta)$.

with a maximum band-gap lowering of ≈ 70 meV occurring for a growth temperature of 670°C (our most ordered epilayer). Figure 6(b) shows the [110] and $[1\bar{1}0]$ absorptive transition energies (as determined by 15 K polarized PLE) as a function of T_g . Note that the energy difference between polarizations is greatest when the band gap is lowest. This is consistent with the theory: the crystal-field splitting is expected to depend on the degree of ordering in the sample.

Figure 7 shows the slope of the rising edge of the PLE spectrum as a function of sample growth temperature T_g , the slope being measured as the energy width of the 10–90% intensity rise. The PLE slope is a measure of the width of the $F(\eta)$ distribution, while the crystal-field splitting (or energy separating between polarizations, discussed in the preceding paragraph) is a measure of η_p in the sample. Using this interpretation we observe that the more ordered samples in this study exhibit a wider statistical distribution of ordered domains than the disordered samples in the range $T_g > 670^\circ\text{C}$. The previous conclusions about the width of the distribution $F(\eta)$ are consistent with a plot of the width of the PL peaks as a function of T_g , as shown in Fig. 8. This figure indicates that the width of the distribution increases with degree of ordering.

IV. CONCLUDING REMARKS

In summary, we have used the spectroscopic techniques of PL and PLE to study the microstructure of spontaneously ordered GaInP₂ grown on (001) GaAs substrates misoriented 2° toward $[0\bar{1}1]$. Data analysis was performed with respect to growth temperature and the resultant band gap, and as a function of sample temperature. Three trends were shown to correlate with ordering: (i) a low-temperature redshift of the PL peak energy with respect to the absorption edge; (ii) a crystal-field-induced polarization of the absorption edge; (iii) a softening of the absorption edge as measured with PLE. These observations provide strong evidence for a statistical distribution of domains in GaInP₂ grown on 2° \rightarrow $[0\bar{1}1]$

misoriented substrates in support of the microstructural model proposed in an earlier paper.¹³ Future work will concentrate on optimization of the growth conditions and substrate misorientation to achieve uniform epilayers that exhibit maximal ordering.

ACKNOWLEDGMENTS

This work was supported by the U.S. Department of Energy, Office of Energy Research, Grant No. DE-AC02-83CH10093.

-
- ¹D. B. Laks, S.-H. Wei, and A. Zunger, *Phys. Rev. Lett.* **69**, 3766 (1992).
- ²R. C. Miller and R. Bhat, *J. Appl. Phys.* **64**, 3647 (1988).
- ³S. Froyen and A. Zunger, *Phys. Rev. Lett.* **66**, 2132 (1991).
- ⁴M. Kondow, S. Minagawa, Y. Inoue, T. Nishino, and Y. Hamakawa, *Appl. Phys. Lett.* **54**, 1760 (1989).
- ⁵J. E. Fouquet, V. M. Robbins, S. J. Rosner, and O. Blum, *Appl. Phys. Lett.* **57**, 1566 (1990).
- ⁶A. Gomyo, T. Suzuki, and S. Iijima, *Phys. Rev. Lett.* **60**, 2645 (1988).
- ⁷J. M. Olson, A. Kibbler, and S. Kurtz, *Proceedings of the 19th IEEE Photovoltaics Specialists Conference* (IEEE, New Orleans, LA, 1987), p. 285.
- ⁸S.-H. Wei and A. Zunger, *Phys. Rev. B* **39**, 3279 (1989).
- ⁹T. Kanata, M. Nishimoto, H. Nakayama, and T. Nishino, *Phys. Rev. B* **45**, 6637 (1992).
- ¹⁰A. Mascarenhas, S. Kurtz, A. Kibbler, and J. M. Olson, *Phys. Rev. Lett.* **63**, 2108 (1989).
- ¹¹M. Kondow, H. Kakibayashi, S. Minagawa, Y. Inoue, T. Nishino, and Y. Hamakawa, *Appl. Phys. Lett.* **53**, 2053 (1988).
- ¹²T. Nishino, Y. Inoue, Y. Hamakawa, M. Kondow, and S. Minagawa, *Appl. Phys. Lett.* **53**, 583 (1988).
- ¹³G. S. Horner, A. Mascarenhas, S. Froyen, R. G. Alonso, K. A. Bertness, and J. M. Olson, *Phys. Rev. B* **47**, 4041 (1993).
- ¹⁴D. J. Mowbray, R. A. Hogg, M. S. Skolnick, M. C. DeLong, S. R. Kurtz, and J. M. Olson, *Phys. Rev. B* **46**, 7232 (1992).
- ¹⁵R. G. Alonso, A. Mascarenhas, S. Froyen, G. S. Horner, K. A. Bertness, and J. M. Olson, *Solid State Commun.* **85**, 1021 (1993).
- ¹⁶S. Minagawa, H. Nakamura, and H. Sano, *J. Cryst. Growth* **71**, 377 (1985).
- ¹⁷S.-H. Wei and A. Zunger, *Appl. Phys. Lett.* **56**, 662 (1990).